

Detecting and Quantifying Xylem Embolism by Synchrotron-Based X-Ray Micro-CT

Martina Tomasella, Francesco Petruzzellis, Sara Natale, Giuliana Tromba, and Andrea Nardini

Abstract

The vulnerability to xylem embolism is a key trait underlying species-specific drought tolerance of plants, and hence is critical for screening climate-resilient crops and understanding vegetation responses to drought and heat waves. Yet, accurate determination of embolism in plant's xylem is challenging, because most traditional hydraulic techniques are destructive and prone to artefacts. Hence, direct and in vivo synchrotron-based X-ray micro-CT observation of xylem conduits has emerged as a key reference technique for accurate quantification of vulnerability to xylem embolism. Micro-CT is nowadays a fundamental tool for studies of plant hydraulic architecture, and this chapter describes the fundamentals of acquisition and processing of micro-CT images of plant xylem.

Key words X-ray, Micro-CT, Xylem vulnerability, Xylem embolism, PLC, Stem, Leaf

1 Introduction

X-ray micro-computed tomography (micro-CT) is a powerful non-destructive imaging technique that allows obtaining information on the internal structure of different samples via the detection of the attenuation or the phase shift of the X-rays transmitted through the sample itself. During a micro-CT scan, the X-ray beam, after passing through the object, is collected by a detector. While the sample is rotating, a sequence of bidimensional projections is taken, usually at a fixed angular increment.

After application of adequate reconstruction algorithms and filtering functions, 3D virtual volumes or virtual cuts (slices) of the sample can be visualized. In the specific case of plants, this technique allows to clearly distinguish gas-filled from water-filled spaces, thus allowing analysing hydraulic integrity and embolism patterns of the xylem conduits [e.g. 1, 2]. So far, micro-CT has been widely used to visualize and quantify xylem embolism because

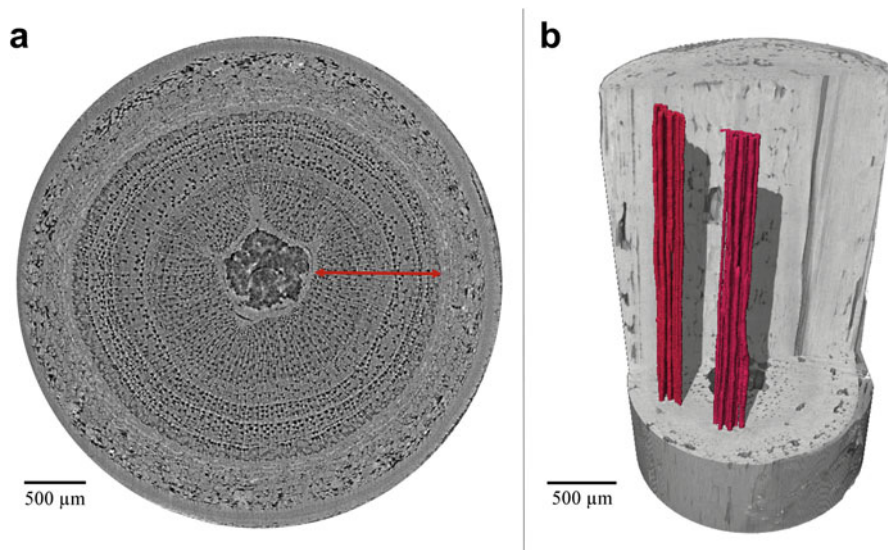


Fig. 1 2D and 3D in vivo visualization by synchrotron-based X-ray Micro-CT of xylem emboli in stems: (a) 2D transverse image of a *Populus nigra* L. stem, and (b) 3D reconstruction of a *Helianthus annuus* L. stem in drought-stressed potted plants. In (a), gas-filled xylem conduits are shown in black in the sapwood region delimited by the red double arrow. In (b), two bundles of reconstructed empty xylem vessels are marked in red

of its high spatial resolution (down to ca. 1 μm pixel size), high signal-to-noise ratio and fast scan times [3–9]. Most importantly, micro-CT allows direct observation of xylem embolism in vivo on intact plants, thus offering significant advantages over classical destructive hydraulic techniques that are potentially prone to artefacts [10–12]. However, it should be noted that X-rays could cause severe damage to living cells [13], and depending on the purpose of the study, special attention should be paid to reduce the delivered radiation dose and sample exposure time and to avoid multiple scans on the same sample.

Micro-CT allows obtaining both transverse two-dimensional (2D) images and three-dimensional (3D) reconstructions of stems, petioles, leaf portions (including veins), and roots. Examples of a 2D and a 3D reconstruction of stems are shown in Fig. 1. While both image types allow detecting xylem embolism, 3D reconstructions provide important information on structural connectivity and heterogeneity of the xylem network [14, 15]. Reconstructed slices offer a simple and reliable tool to detect gas-filled conduits, while also allowing easy measurements of conduit size. Thus, these images are used to estimate the theoretical xylem hydraulic conductivity and percentage loss of hydraulic efficiency due to embolism accumulation. By observing the xylem in plants or plant samples of the same species at different hydration levels, it is also possible to relate the percentage of embolized conduits to the xylem pressure, thus constructing xylem vulnerability curves to estimate hydraulic vulnerability parameters (e.g., the water potential inducing 50% loss

of hydraulic conductivity, Ψ_{50}) that can also be estimated with classical hydraulic methods [4]. This allows to validate the classical hydraulic measurements, which are potentially prone to artefacts.

In this chapter, we illustrate a method to analyse xylem embolism using 2D images acquired by synchrotron-based X-ray micro-CT. We describe how this method can be applied to different plant organs both in vivo (intact plants) and ex vivo (cut plant portions).

2 Materials

2.1 Synchrotron-Based Micro-CT Facility

1. Synchrotron radiation laboratory with phase contrast imaging (PCI) approach (see Subheading 3.1 for detailed description). See **Note 1** for information on facilities availability.

2.2 Plant Material

1. Intact plants/cut plant portions (*see Note 2*).

2.3 Sample Preparation

1. Wooden sticks with a screw at the bottom that can be mounted on the sample holder are required to keep eventual bending-prone samples in a vertical position (*see Note 3*) (Fig. 2).
2. Parafilm.
3. Cling film.
4. Adhesive tape (e.g., American tape).
5. Plastic bags to contain eventual pots, root systems, and soil to avoid soil particles loss.
6. Razor blades and scissors.

2.4 Additional Measurements

1. A Scholander pressure chamber (alternatively a dewpoint hygrometer or a leaf/stem psychrometer) to measure leaf or stem water potential (Ψ_{leaf} and Ψ_{stem} , respectively).
2. A razor blade to cut the petiole/base of the leaf.
3. Cling film to wrap the leaf used for Ψ_{leaf} or Ψ_{stem} determination.
4. A light source and a stereoscope/magnifying lens to examine the cut section of the leaf blade/petiole/stem and to detect sap appearance during progressive pressurization of the sample.

2.5 Reconstruction Software

1. Reconstruction software for X-ray micro-CT data (see Subheading 3.5 for explanations).

2.6 Image Analysis Software for Xylem Embolism Quantification

1. ImageJ [16] (a free and complete tool for image visualization, but also commercial image analysis software are available).

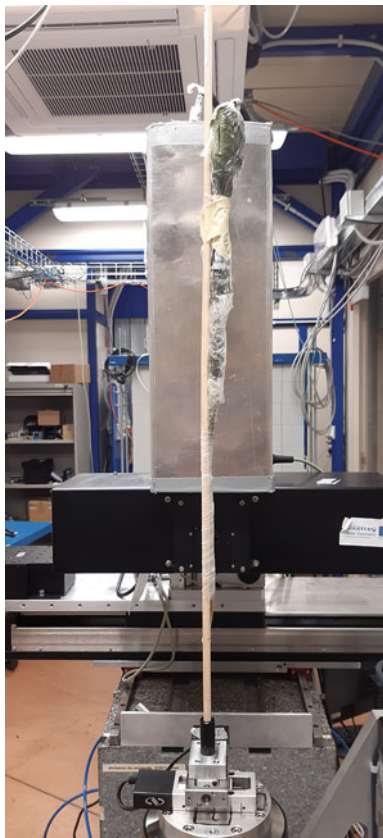


Fig. 2 Example of a cut plant shoot mounted on the sample holder in the X-ray micro-CT setup at the SYRMEP beamline of the Elettra synchrotron facility. In this setup, the sample holder consists of a ca. 1 m wooden stick fixed at the base to a plastic cylinder, directly screwed on the rotator

3 Methods

3.1 *Technical Specification*

Conventional micro-CT facilities are based on micro-focus X-ray generators. Like all X-ray tubes, these sources produce X-rays when highly energetic electrons are stopped in a solid metal anode. A polychromatic conic beam is generated, from which a conical solid angle is selected. Many benchtop micro-CT systems are nowadays able to reach very high-resolution level, in the range of 1 μm with a voxel size even below 1 μm . The position of the sample with respect to the source and the detector can be changed to adjust the magnification and the resolution. However, as the sample must stay inside the field of view, the optimal position is always a compromise between sample size and spatial resolution. The mainly used technique is the absorption modality as the produced beam is not always enough coherent to obtain phase contrast.

A new generation of X-ray sources based on the liquid-metal-jet anode (MetalJet) technology has been recently implemented to improve the limitations of conventional systems with an important increase in the brightness. With these systems, a sufficient grade of spatial coherence is achieved, allowing the use of phase-contrast imaging techniques. However, for these sources the available X-ray fluxes are still far below the ones available at synchrotron labs. As a consequence, the time required to complete a CT scan in phase contrast modality is much longer.

Synchrotron radiation (SR) is generated by an electron traveling at relativistic speed when it changes movement direction. SR covers a large spectrum of electromagnetic waves, from infrared to hard X-rays. SR is produced in large accelerator-based facilities equipped with different magnetic structures (bending magnets and insertion devices) optimized to maximize radiation production for the different experimental purposes and user requirements. SR is extracted from the accelerators and transported to the experimental stations through so-called *beamlines*.

The peculiar properties of SR, such as the high spatial coherence of the source, the monochromaticity, and the high available fluxes, have opened unprecedented opportunities in the field of hard X-ray imaging. In this framework, the phase contrast imaging (PCI) techniques have been developed with the aim of improving the image quality available from conventional sources, and overcoming their main limitations in the study of soft biological tissues. Image contrast, which in conventional imaging is due to differences in the X-ray absorption, has been overcome by the information of phase shifts occurring to the coherent X-rays crossing the sample and determining the phase contrast in the image. This implied a real revolution in biomedical and biological X-ray imaging that involved wide application areas at different resolution scales. For imaging plants vascular system, the use of PCI approach is fundamental as it allows to easily visualize a gas phase even in very narrow xylem conduits, thus facilitating image segmentation and a quantitative assessment of embolism.

Before mounting the sample on the sample holder placed in the hutch, the user must set the following technical details related to the observation and acquisition procedure.

Based on the specific research question, the user has first to define the average X-ray source energy, and thus apply proper filters between the beam exit point and the sample to eventually decrease beam's energy to the desired level. As an example, in Savi et al. [5], two filters (1 mm of aluminium and 1 mm of silicon) were used to obtain an average X-ray source energy of 22 keV. Common energy levels used to image xylem embolism range from 20 to 25 keV.

In a second step, the sample-to-detector distance and the zoom of the detector must be set up according to the desired pixel size, which must consider xylem conduit diameter and the sample size (*see Note 4*), as well as the available field of view (FOV).

3.2 How to Prepare Plant Samples

While observation of different organs in intact plants provide a reliable estimate of xylem embolism, the use of cut plant portions can lead to experimental artefacts similar to those observed in some classical hydraulic techniques. In this case, care should be taken during sample preparation to avoid “open vessel artefacts” when using stem/branch segments shorter than maximum vessel length [12, 17] and spurious embolism generation when cutting xylem under tension [10, 11], as both can potentially lead to embolism overestimation. The size of intact plants that can be observed at the beamline is often limited by the design and features of the sample holder and of the detector. While some facilities allow observations of relatively big plants rooted in large and heavy pots (up to 60 kg), most commonly the reasonable plant size is limited to about 1 m height. A new setup optimized for the study of heavy samples has been recently implemented at the SYRMEP beamline [18] and will allow to perform accurate microCT studies on plants with bigger stem sizes (5–10 cm).

1. Roots/pots are tightly enclosed in plastic bags to avoid soil losses to the mechanisms of the rotator/sample holder. In this way, the plant can also be mounted upside-down, allowing scanning of apical vs basal parts. For intact plants, it could be necessary to partially remove the soil before the scan when the available sample holder cannot sustain the weight of the pot. The stem and, most importantly, the leaves must be also wrapped in cling film to avoid water loss during the scan. Parafilm and tape are used to properly attach the sample to the wooden/plastic stick, in order to avoid sample’s swinging during the sample rotation.
2. The scanned portion is attached to the wooden stick with parafilm.
3. The stick is fixed to the sample holder on the rotator. The plant (with the stick) is mounted on the sample holder taking care that the stem is vertically oriented, and when rotating, the part to be scanned remains on the rotation axis and perpendicular to the beam.

3.3 Acquisition Procedure

The image acquisition is performed using a specific software controlling the detector and all the motion stages for sample positioning. Before launching the acquisition, it is necessary to select the X-ray energy, the exposure time, and the number of projections. In the nearby parallel geometry of the SR X-ray beam, the CT scan is performed with a total rotation angle of 180°. A rotation over 360° can be used to extend the detector field of view. Indeed, in the so-called half acquisition mode, an off-center rotation over 360° is performed to almost double the width of the available field-of-view [19].

The total exposure time determines the entrance dose delivered to the sample. The dose has to be carefully evaluated in order to reduce the sample damage and must be set according to the specific research question (*see Note 5*). For example, in Secchi et al. [9], 1800 projections were acquired at an exposure time of 100 ms with a 360°-degree rotation angle, resulting in a total acquisition time of 3 min and in an entrance dose rate in water of 47 mGy s⁻¹. Typical scan times for different studies performed at synchrotron facilities range from 75 s to 4 min.

Dark and flat images must be acquired prior to sample scanning (*see Note 6*). For dark images, it is necessary to launch an acquisition while the beam is off. For flat images, acquisition must be launched after the beam is turned on and after moving the sample outside the FOV.

After these preliminary acquisitions, the sample is placed in the centre of the FOV and the acquisition can start (*see Note 7*).

Additionally, according to the research question, the above steps could be repeated after cutting the samples few mm above the scanned area to induce embolism in all functional conduits. This is often necessary as water-filled conduits cannot be easily recognized against the background of hydrated parenchyma and mechanical cells of the wood, so that it might be impossible to calculate the embolism rate as a percentage of embolized conduits over the total number of conduits. Furthermore, this final cutting procedure allows to distinguish mature and functional conduits from immature ones, thus improving the accuracy of embolism estimation (see Subheading 3.6).

After saving sample's acquisition, the sample is removed from the sample holder and used for eventual additional measurements.

3.4 Additional Measurements

The quantification of xylem embolism is usually coupled with measurement of leaf or stem water potential (Ψ_{leaf} and Ψ_{stem} , respectively). For each sample, Ψ_{leaf} is measured on mature and fully expanded leaves. For Ψ_{stem} determination using the pressure chamber, leaves must be wrapped in cling film to equilibrate Ψ_{leaf} with Ψ_{stem} at least 30 min before measurement. Here, below, are the procedures to be applied for each of the instruments for water potential determination:

1. Pressure chamber: Excise the leaf from the stem and wrap it immediately in plastic film (*see Note 8*). Remove few mm of the petiole with a razor blade, making a couple of close and perpendicular cuts. Place the leaf in the pressure chamber, and apply gas pressure inside the chamber until sap emerges from xylem [20]. For best procedures, see methodological tests performed by Rodriguez-Dominguez et al. [21].
2. Dewpoint hygrometer: After calibrating the instrument (check instrument manual for the calibration procedure), cut leaf discs

or stem segments according to the size of the sample holder and place them in the measurement chamber. For some leaves, it could be necessary to punch the blades with a needle to favour water potential equilibration during measurements. In the case of stems, split them longitudinally before inserting them in the chamber.

3. Leaf/stem psychrometer: Calibrate the instrument according to the calibration procedure of the specific instrument. Leaf/stem surface must be cleaned and dried prior sealing the portion of the sample in the psychrometer. Abrade surface of leaf/stem, apply some silicon grease around psychrometer surface, place the sample into a sealed chamber, and allow it to equilibrate.

3.5 Image Reconstruction

The reconstruction workflow of X-ray micro-CT data is based on multiple computational steps, from flat fielding and the application of conventional filtered back projection (FBP) algorithm [22] to more refined image processing to compensate artefacts, enhance the quality of the reconstructed images and improve the identification of the different structures. To this aim, additional preprocessing algorithms are used in phase contrast imaging to decouple phase from absorption effects and improve image contrast [23]. In this light, an open-source software package, namely, SYRMEP Tomo Project (STP) [24], has been developed to allow the users of SYRMEP beamline at Elettra synchrotron designing custom CT reconstructions. The software is free to use, and its releases can be downloaded at the Elettra Scientific Computing group GitHub repository <https://github.com/ElettraSciComp/STP-Gui>. Commercial software is also available on the market.

Generally, the output of the acquisition process is a file under a format (e.g., TDF, Tomo Data Format) that allows handling a large dataset consisting in a sequence of 2D image files (usually a TIFF file for each acquired projection as well as flat/dark images). Thus, a software is required to extract and reconstruct the acquired projections in a sequence of 2D images that can be further analysed using image analysis software (see below). The choice of the software depends on the algorithm used for the reconstruction. The simplest one, namely, the filtered back projection (FBP) algorithm after the flat fielding of the projection data, can be run by most of the computing software tools (e.g., MATLAB, IDL) [24]. However, thanks to the coherence of the synchrotron radiation, phase-contrast imaging can be applied on synchrotron-derived data, as it allows differentiating between two materials of similar electron density or with negligible X-ray absorption (i.e., phase objects) so as to ease the image segmentation step and the subsequent analyses [24]. In this light, STP software reconstructs 2D images sequence from TDF files by implementing phase-contrast imaging algorithms.

The framework implemented in the software includes the following steps:

- Preprocessing: In this step, it is possible to apply dark/flat correction, as well as ring removal method;
- Phase-retrieval: In this step, a phase retrieval algorithm [23] can be applied to separate phase from absorption effects and accounting for pixel size, detector-to-sample distance, X-ray energy, and the different attenuation properties of the elements composing the imaged object (i.e., by tuning δ and β coefficients).
- Image reconstruction: This is the step leading to the final reconstruction of the 2D images sequence. Here, the centre of rotation could be automatically calculated or manually inserted if known and the reconstruction algorithm can be specified.
- Postprocessing: This step allows to set several features of the reconstructed 2D image sequences, such as rescaling images to 8- or 16-bit quality or to select a region of interest to be reconstructed.

3.6 Image Analysis

Reconstructed 2D transverse section images are analysed via an image analysis software. Hereafter, the procedure for ImageJ is described. The proper scale is set based on pixel size (image -> set scale). The sapwood area on which performing the measurements (from vascular cambium to pith excluded) is selected with the polygon selection tool (*see Note 9*) and measured (analyze -> measure).

In the selected sapwood area, a proper pixel threshold is selected to clearly identify gas-filled conduits shown in dark grey (Image -> Adjust -> Threshold). Preprocessing adjustments (brightness, contrast) or manual cleaning of the image can be applied to improve the analysis (*see Note 10*).

With the particle analysis tool (image -> analyse particles), the single embolized conduits are identified and counted and their area is measured. The equivalent circle diameter (d) is calculated from single conduit surface areas. Different parameters can be used as an estimate of the amount of xylem embolism.

1. Theoretical percentage loss of hydraulic conductance (PLC_t). Theoretical hydraulic conductance of gas-filled conduits (k_{gf}) is calculated according to the Hagen-Poiseuille Equation from d values, as $(\pi\rho/128\mu)\Sigma d^4$, where ρ and μ are the density of the fluid and the viscosity of water, respectively [25]. The sum of gas-filled and water-filled conduit conductance gives the maximum hydraulic conductance (k_{max}), when it is possible to clearly identify water-filled conduits. Alternatively, k_{max} is calculated from all empty conduits of the transverse section obtained from a second scan done after cutting the stem closely

above the previously scanned area (see Subheading 3.3). k_{gf} and k_{max} can be divided by the cross-sectional xylem area to obtain the theoretical specific hydraulic conductance of gas filled conduits (k_s) and theoretical specific maximum hydraulic conductance (k_{s_max}), respectively. PLC_t is finally calculated as $k_s/k_{s_max} \times 100$ (see **Note 11**).

2. Embolized conduit fraction. This is the number of empty xylem conduits divided by total number of conduits.
3. Embolized sapwood area (A_{embol}). This is calculated by dividing the total embolized pixel area by the mature sapwood area, in percentage. If the reconstructed image of the sample after cutting the stem above the scanned area is available, it is possible to calculate the embolized vessel area (EVA), calculated dividing A_{embol} by the embolized sapwood area, after the final cut made above the scanned region (namely, A_{embol_cut} , see Subheading 3.3), expressed in percentage.

3.7 Xylem Vulnerability Curve (VC) Estimation

Xylem vulnerability curves can be obtained by plotting PLC_t versus the corresponding Ψ_{leaf} or Ψ_{stem} and fitting sigmoidal or Weibull functions using a data analysis software (e.g., MATLAB, Sigmaplot, R) (see **Note 12**). Alternatively, A_{embol} can be used instead of PLC_t , given that the resulting VCs typically show good agreement with those obtained with PLC_t [9]. Depending on the function used, several parameters are obtained. The most important ones from an agronomical and ecophysiological point of view are the water potential at 12, 50, and 88% PLC_t (or A_{embol} , or EVA), namely, Ψ_{12} , Ψ_{50} and Ψ_{88} , respectively.

4 Notes

1. Several synchrotron radiation laboratories are available in Europe, Asia, Australia, and the Americas. The access to imaging beamlines in these laboratories is free of charge and subject to submission of a specific proposal, where the scientific case is presented, the need for SR is justified and a given number of beamtime hours is requested according to the number of samples to be scanned and an estimate of total exposure time needed for each scan. The proposals are evaluated by independent review panels twice a year, and beamtime is assigned according to a merit score. As an example, access to the SYR-MEP imaging beamline at the Elettra synchrotron source (<https://www.elettra.eu/>) is performed through the so called Virtual User Office (<https://vuo.elettra.eu/>). Useful suggestions on how to write a successful proposal are reported in <https://www.elettra.eu/userarea/apbt.html>.

2. Xylem embolism can be quantified on intact plants or cut plant portions, as well as on different plant organs (stems, leaves, petioles, roots), according to the specific research question and to the beamline's technical characteristics (e.g. sample holder, pixel size, field of view). We suggest carefully assessing the size and the weight of intact plants or cut plant portions to be scanned prior the experiments, and in particular to check:
 - (a) Size of the hutch: Very long samples might not fit in the hutch.
 - (b) Characteristics of the sample holder, making sure that the sample's weight can be sustained by the sample holder.
 - (c) Field of view, making sure that at least half of the cross-section of the scanned samples lies within the available field.
3. Wooden sticks are recommended because of their low X-ray absorption and should be adequately tall and hard enough to avoid sample swinging during image acquisition. To easily distinguish the stick from the stem of the sample, a thin metal wire can be rolled around the stem, right above or below the region to be scanned (*see* also **Note 7**).
4. Pixel size must be lower than xylem conduit diameter. For example, in Losso et al. [6], the pixel size was set to 2 μm and conduit diameter of the study species ranged between 15 and 25 μm .
5. Carefully choose exposure time: not too fast to avoid plant movement or oscillations during rotation, and not too slow to prevent samples receiving an excessive X-ray dose.
6. The number of projections and the exposure time could be reduced for dark and flat acquisition, in order to reduce the total acquisition time.
7. Make sure that samples (or the region that must be acquired) during the rotation are centred and do not move out of the FOV. The centre of rotation could be checked during sample preparation by placing 1 mm long metal wire few millimetres above the scanning area. In live mode, it will be clearly visible by the detector. To assess whether the sample is centred in the FOV, let it rotate by 180° and be sure that the steel wire remains in the centre of rotation.
8. This is fundamental to prevent water loss during sample preparation.
9. If stem sapwood is larger than the field of view and, therefore, only a part of the sapwood is imaged, analyses are done on a smaller portion.

10. Manual selection of conduits may be necessary. In this case, the ROI menu in ImageJ is a helpful tool.
11. Note that here k_s is the theoretical specific hydraulic conductance of gas filled conduits, so the formula differs from that used for classic hydraulic measurements, where the initial (native) k is the specific hydraulic conductance of water filled conduits.
12. “fitplc” R package [26] is widely used.

References

1. Brodersen CR, McElrone AJ, Choat B et al (2013) In vivo visualizations of drought-induced embolism spread in *Vitis vinifera*. *Plant Physiol* 161:1820–1829
2. Choat B, Brodersen CR, McElrone AJ (2015) Synchrotron X-ray microtomography of xylem embolism in *Sequoia sempervirens* saplings during cycles of drought and recovery. *New Phytol* 205:1095–1105
3. Cochard H, Delzon S, Badel E (2015) X-ray microtomography (micro-CT): a reference technology for high-resolution quantification of xylem embolism in trees. *Plant Cell Environ* 38:201–206
4. Nardini A, Savi T, Trifilò P, Lo Gullo MA (eds) (2017) Drought stress and the recovery from xylem embolism in woody plants, *Progress in botany*, vol 79. Springer, Cham, pp 197–231
5. Savi T, Miotto A, Petruzzellis F et al (2017) Drought-induced embolism in stems of sunflower: a comparison of in vivo micro-CT observations and destructive hydraulic measurements. *Plant Physiol Biochem* 120:24–29
6. Losso A, Bär A, Dämon B et al (2019) Insights from in vivo micro-CT analysis: testing the hydraulic vulnerability segmentation in *Acer pseudoplatanus* and *Fagus sylvatica* seedlings. *New Phytol* 221:1831–1842
7. Peters JMR, Gauthey A, Lopez R et al (2020) Non-invasive imaging reveals convergence in root and stem vulnerability to cavitation across five tree species. *J Exp Bot* 71:6623–6637
8. Tomasella M, Casolo V, Natale S et al (2021) Shade-induced reduction of stem nonstructural carbohydrates increases xylem vulnerability to embolism and impedes hydraulic recovery in *Populus nigra*. *New Phytol* 231: 108–121
9. Secchi F, Pagliarani C, Cavalletto S et al (2021) Chemical inhibition of xylem cellular activity impedes the removal of drought-induced embolisms in poplar stems – new insights from micro-CT analysis. *New Phytol* 229: 820–830
10. Wheeler JK, Huggett BA, Tofte AN et al (2013) Cutting xylem under tension or supersaturated with gas can generate PLC and the appearance of rapid recovery from embolism. *Plant Cell Environ* 36:1938–1949
11. Trifilò P, Raimondo F, Lo Gullo MA et al (2014) Relax and refill: xylem rehydration prior to hydraulic measurements favours embolism repair in stems and generates artificially low PLC values. *Plant Cell Environ* 37: 2491–2499
12. Torres-Ruiz JM, Jansen S, Choat B et al (2015) Direct X-ray microtomography observation confirms the induction of embolism upon xylem cutting under tension. *Plant Physiol* 167:40–43
13. Petruzzellis F, Pagliarani C, Savi T et al (2018) The pitfalls of in vivo imaging techniques: evidence for cellular damage caused by synchrotron X-ray computed micro-tomography. *New Phytol* 220:104–110
14. Brodersen CR, Lee EF, Choat B et al (2011) Automated analysis of three dimensional xylem networks using high-resolution computed tomography. *New Phytol* 191:1168–1179
15. Wason J, Bouda M, Lee EF et al (2021) Xylem network connectivity and embolism spread in grapevine (*Vitis vinifera* L.). *Plant Physiol* 186: 373–387
16. Schneider CA, Rasband WS, Eliceiri KW (2012) NIH image to ImageJ: 25 years of image analysis. *Nat Methods* 9:671–675
17. Martin-StPaul NK, Longepierre D, Huc R et al (2014) How reliable are methods to assess xylem vulnerability to cavitation? The issue of “open vessel” artifact in oaks. *Tree Physiol* 34: 894–905
18. Dullin C, D’Amico L, Saccomano G et al (2023) Novel setup for rapid phase contrast CT imaging of heavy and bulky specimens. *J*

- Synchrotron Rad 30:650. <https://doi.org/10.1107/S1600577523001649>
19. Buzug TM (2008) Computed tomography: from photon statistics to modern cone-beam CT. Springer, Berlin/Heidelberg
 20. Brown PW, Tanner CB (1981) Alfalfa water potential measurement: a comparison of the pressure chamber and leaf dew-point hygrometers. *Crop Sci* 21:240–244
 21. Rodriguez-Dominguez CM, Forner A, Martorell S et al (2022) Leaf water potential measurements using the pressure chamber: synthetic testing of assumptions towards best practices for precision and accuracy. *Plant Cell Environ* 45:2037. <https://doi.org/10.1111/pce.14330>
 22. Kak AC, Slaney M (1988) Principles of computerized tomographic imaging. IEEE Press, New Brunswick
 23. Paganin D, Mayo SC, Gureyev TE et al (2002) Simultaneous phase and amplitude extraction from a single defocused image of a homogeneous object. *J Microsc* 206:33–40
 24. Brun F, Pacilè S, Accardo A et al (2015) Enhanced and flexible software tools for X-ray computed tomography at the Italian synchrotron radiation facility Elettra. *Fundamenta Informaticae* 141:233–243
 25. Tyree MT, Zimmermann MH (2002) Xylem structure and the ascent of sap. Springer, Berlin/Heidelberg
 26. Duursma R, Choat B (2017) fitplc – an R package to fit hydraulic vulnerability curves. *J Plant Hydraul* 4:e002